JOURNAL OF GEOPHYSICAL RESEARCH, VOL. 115, B02402, doi:10.1029/2007JB005475, 2010

Mechanics of the giant radiating Mackenzie dyke swarm: A paleostress field modeling

Guiting Hou,[1] T. M. Kusky,[2] Chuancheng Wang,[1] and Yanxin Wang[1]

Received 31 October 2007; revised 31 May 2009; accepted 21 September 2009; published 4 February 2010.

[1] The 1.27 Ga Mackenzie dyke swarm of the Canadian Shield is a giant radiating dyke swarm that gradually swings in orientation from N-S in the focal area to NW-SE trends in peripheral areas. In this paper, we propose a new model (the "Plug" model) that accounts for the paleostress contribution to the mechanism of emplacement for the Mackenzie dyke swarm in the Canadian Shield. The 1.27 Ga stress field on the Canadian Shield calculated by the "Plug" model explains the radiating nature of the Mackenzie dyke swarm around the Coppermine River lava field by local stress concentrations. The parallel nature of the dyke swarm at distance (more than 1000 km) from the focal source can be explained by the existence of a regional tectonic stress field created by ridge push acting on the southeast margin of the Canadian Shield from the Grenville Ocean. The thin elastic plate and two-dimensional cross-section modeling suggest that the interaction between stresses from a mantle upwelling and the Grenville Ocean spreading play an important role in the intrusion mechanism of the Mackenzie dyke swarm. The change in dyke orientation from N-S trending to NW-SE trending is caused by coupling between resistance from the focal area (Plug area) and a Grenville Ocean ridge push.

Citation: Hou, G., T. M. Kusky, C. Wang, and Y. Wang (2010), Mechanics of the giant radiating Mackenzie dyke swarm: A paleostress field modeling, *J. Geophys. Res.*, *115*, B02402, doi:10.1029/2007JB005475.

1. Introduction

[2] The Precambrian stress field of an Archean craton is very difficult to reconstruct because few paleostress indicators remain. Mafic dyke swarms represent conspicuous extensional structures and are widespread in cratons throughout the world. Mafic dykes are excellent time markers and paleostress indicators, and can be used to reconstruct the paleostress fields of cratons and supercontinents. In general, dyke swarms (with tensional forms) exhibit trends parallel to the contemporaneous regional horizontal maximum compressive stress direction and perpendicular to the extension direction [*Pollard*, 1987; *Baer and Beyth*, 1990; *Hoek and Seitz*, 1995; *Gudmundsson*, 1995; *Heeremans et al.*, 1996]. Undeformed and unmetamorphosed dyke swarms can be regarded as observable paleostress indicators in Precambrian cratons [*Pollard*, 1987; *Hou et al.*, 2006]. Parallel dyke swarms form in response to a regional stress field, for example, the mafic dyke swarms in the North China Craton [*Hou et al.*, 2006], while radiating dyke swarms may form due to stress concentrations around a plutonic or volcanic edifice, as in the case of the radiating dyke swarm at Spanish Peak, USA [*Smith*, 1987]. The mechanics of the radiating and parallel dyke swarms are supported by theoretical and experimental studies [*Rickwood*, 1990; *Gudmundsson*, 2006]. Fractures that formed prior to magmatism may also play a role in dictating dyke swarm geometry, though the exact mechanism of dyke propagation is still controversial [*Dehls et al.*, 1998; *Acocella et al.*, 2003; *Valentine and Krogh*, 2006]. In most cases, preexisting fractures are induced by tectonic stresses and not by magma injection, though magma injection can increase fracture size by fracture propagation at the dyke tip [*Pollard*, 1987].

[3] The Mackenzie dyke swarm of the Canadian Shield forms a 2100 km long swarm of radiating dykes around a focal source centered on the Coppermine Lava field of the Canadian Arctic (Figure 1). However, with increasing distance from the source, the dyke orientations swing from N-S to NW-SE and the dyke swarm adopts the geometry of a parallel dyke swarm [*Baragar et al.*, 1996; *Ernst and Buchan*, 1999] (Figure 1). To date, no numerical simulation has been done for the mechanics of the Mackenzie dyke swarm; however, previous studies [*Ernst and Baragar*, 1992; *Ernst et al.*, 1995] suggest that the Mackenzie dyke swarm formed in response to the arrival of a mantle plume beneath the focal area (Coppermine River lava field).

[4] At the Earth's free surface, dykes mostly fill extensional fractures. The trends of the dykes follow the direction of the horizontal maximum principal compressive stress, σ_{Hmax}, and are perpendicular to the direction of the horizontal minimum principal stress, σ_{Hmin} [*Pollard*, 1987; *Baer and Beyth*, 1990; *Hoek and Seitz*, 1995; *Gudmundsson*, 1995, 2002; *Heeremans et al.*, 1996]. *Ernst and Buchan* [1999] proposed that the orientations of the Mackenzie and Sudbury dyke swarms reflect the stress pattern of the Canadian Shield

[1] Key Laboratory of Orogenic Belts and Crustal Evolution, School of Earth and Space Sciences, Peking University, Beijing, China.
[2] Three Gorges Geohazards Research Center, and State Key Lab for Geological Process and Mineral Resources, China University of Geosciences, Wuhan, China.

0148-0227/10/2007JB005475$09.00

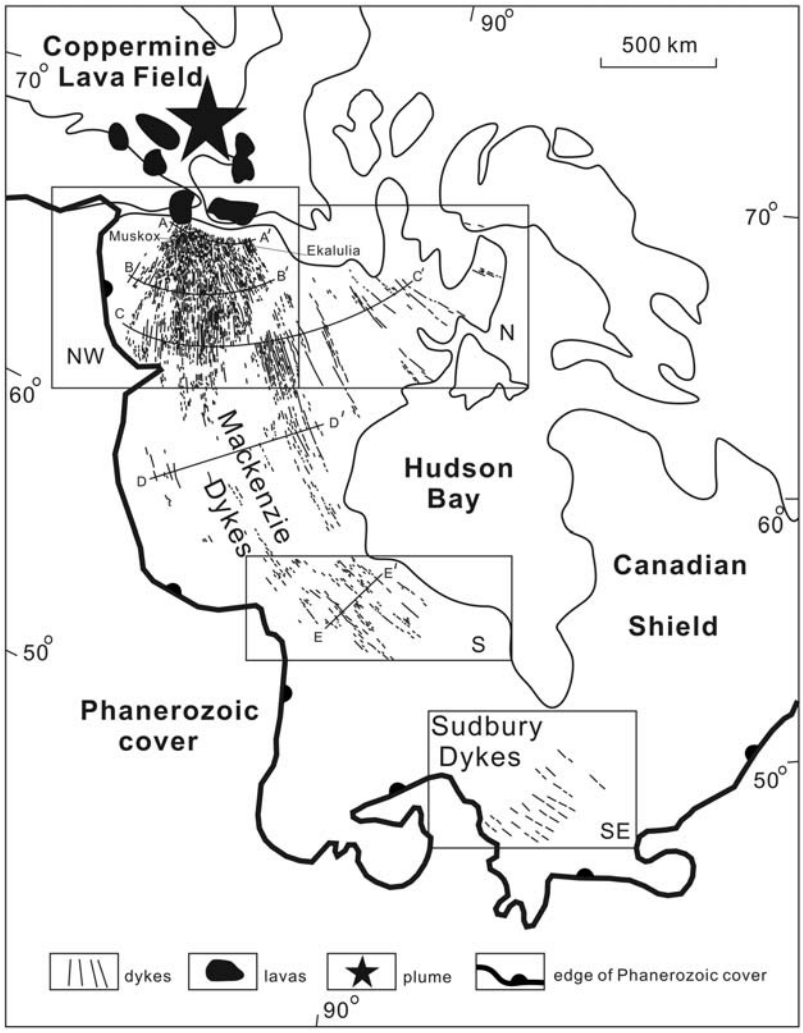

Figure 1. Distribution of the giant radiating Mackenzie mafic dyke swarm (sources: *Gibson et al.* [1987], *Baragar et al.* [1996], and *Ernst and Buchan* [1999]).

from 1267 to 1240 Ma, and that the NW-SE regional horizontal maximum compressive stresses indicated by the dyke orientations are consistent with the Grenville Ocean opening or back-arc spreading at this time, but that dramatically radiating orientations of dykes around the focal area in the NE Canadian Shield required a different stress regime. *Ernst and Buchan* [1999] suggested that the orientation of the parallel dyke swarms on the Canadian Shield reflect the orientation of the regional horizontal maximum stress at the time of their formation, but they did not provide a numerical model for the mechanism of intrusion of the Mackenzie dyke swarm and transition of dyke orientations from N-S to NW-SE to support these ideas.

[5] The preexisting "Hole" model for the formation of radiating dyke swarms can account for the formation of small-scale radiating dyke swarms [*Gudmundsson*, 2006] (Figure 2a), but does not explain the size of the giant radiating dyke swarms nor the origin of changes in dyke swarm orientation with distance from the focal area. In this paper, we propose a "Plug" model based on the results of elastic thin plate and two-dimensional elastic section finite element modeling to explain the mechanics of the Mackenzie dyke swarm (Figure 2b). Our model explains the development of radiating dykes concentrated around the focal area and orientation change of parallel dykes far from the magma source during opening of the Grenville Ocean [*Davidson*, 1995, 1998].

2. Geological Setting

[6] The Canadian Shield consists of a number of Archean cratons: the Superior (Superior and Southern provinces), Wyoming, Slave, Nain, and Churchill (Hearne, Rae, and Burwell domains). These cratons have been sutured by collisional orogenesis (e.g., Wopmay, Taltson-Thelon, Trans-Hudson, New Quebec, and Torngat orogens) between 2.0 and 1.8 Ga [*Hoffman*, 1989; *Van Kranendonk et al.*, 1993] (Figure 3). It is thought that Greenland was attached to North America from the late Archean until the opening of the Labrador Sea (between North America and Greenland) in the Late Mesozoic [*Roest and Srivistava*, 1989] or Early Cenozoic [*Chalmers and Laursen*, 1995]. The Archean rocks within the Superior, Rae, Hearne, and Slave cratons are composed predominantly of 3.0–2.6 Ga greenstones, granites, high-grade gneisses, and metasedimentary rocks [*Hoffman*, 1989; *Kusky and Vearncombe*, 1997]. The orogens surround-

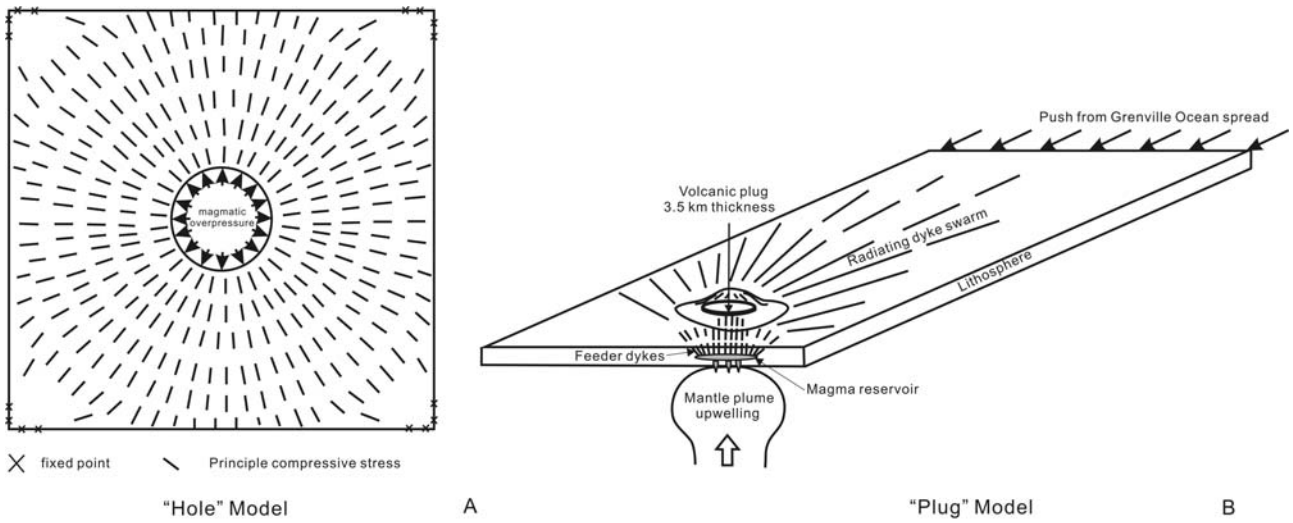

Figure 2. Two thin elastic plate models for the mechanism of the Mackenzie dyke swarm (a) "Hole" model after *Gudmundsson* [2006] and (b) "Plug" model proposed in this paper.

ing the cratons of the Canadian Shield are composed of 3.0–2.8 Ga reworked basement, Paleoproterozoic metamorphic volcanic and sedimentary rocks and granitic plutons [*Windley*, 1992; *Grover et al.*, 1997; *Kusky and Polat*, 1999]. Additionally, a 1.8–1.3 Ga magmatic accretionary zone extends from Arizona through Colorado and Michigan, bordering the southern margin of the Canadian Shield [*Gower et al.*, 1990; *Park*, 1992; *Karlstrom et al.*, 2001]. Petrological and geochemical studies indicate that this large magmatic belt includes dominantly juvenile volcanogenic sequences and granitoid suites [*Hoffman*, 1989; *Windley*, 1992; *Park*, 1992].

[7] Along the southeastern margin of the Canadian Shield, the Grenville Orogen records an about 300 Ma history of orogenesis, culminating in arc-continent and continent-continent collision between about 1150 and 1120 Ma, continuing until about 980 Ma [*Davidson*, 1995, 1998]. The Grenville Ocean along the southeastern margin of the Canadian Shield would have been comparable to the present Pacific Ocean with island arc/terrane accretion occurring during Mesoproterozoic times between 1.3 and 1.2 Ga [*Hoffman*, 1989, 1991; *Davidson*, 1995, 1998; *Kusky and Loring*, 2001].

[8] The Mesoproterozoic Mackenzie igneous events in the Canadian Shield comprise one of the most widespread episodes of mafic magmatism recorded in continental crust. The Mackenzie dykes fan out in a radial array (about 100° of arc) that extends for more than 2100 km along strike and has a maximum width of 1800 km. The areal extent of the Mackenzie dyke swarm is about 2,700,000 km^2 [*Ernst et al.*, 1995] (Figure 1).

[9] The huge, fan-shaped Mackenzie mafic dyke swarm is distributed over more than half of the Canadian Shield and converges toward a focal point where a region of coeval volcanic and plutonic activity is represented by the Coppermine River-Ekalulia basalts and the Muskox layered intrusion. Precise U-Pb baddeleyite ages indicate that the Muskox intrusion, Coppermine-Ekalulia basalts, and the Mackenzie dyke swarm were all emplaced within a period of less than 5 million years beginning at 1272 Ma [*Le Cheminant and Heaman*, 1989]. The age of a pyroxenite from the layered

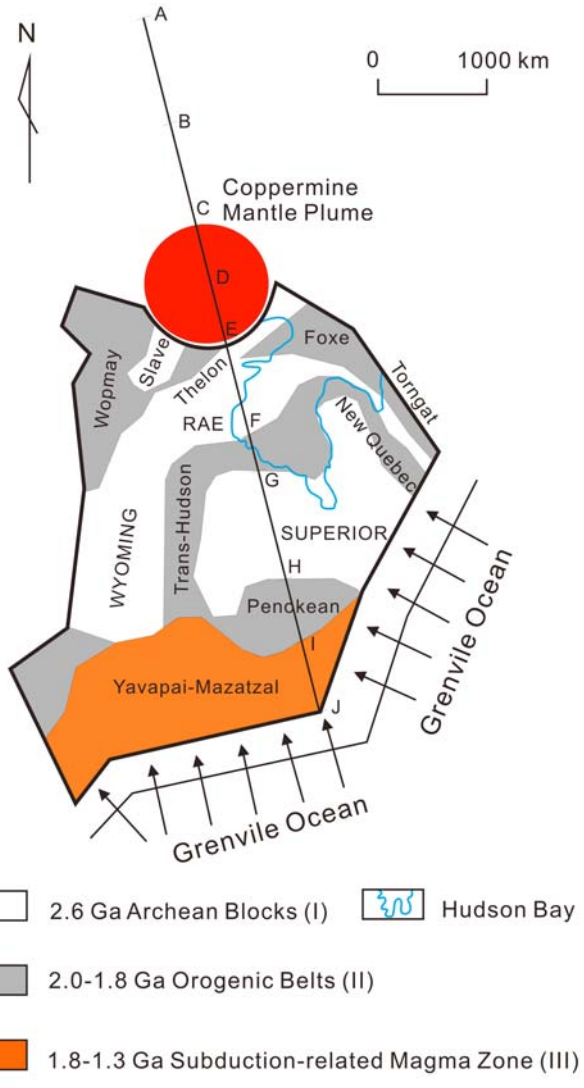

Figure 3. Tectonic model of the Canadian Shield and its Precambrian tectonic divisions.

Survery lines	Length of the survey lines (m)	Average width of dyke (m)	Number of dykes	Extension ratio (%)	Rose diagrams dominant strikes	Radiating province or parallel province
AA'	370,000	30	55	0.45	N (10°-30°)	Radiating province
BB'	650,000	30	70	0.32	N (0°-10°)	Radiating province
CC'	1,300,000	30	93	0.21	N (350°-360°)	Radiating province
DD'	750,000	30	15	0.06	N (350°-360°)	Parallel province
EE'	300,000	30	12	0.12	N (320°-330°)	Parallel province

The extension ratios arrange between 0.06%-0.45%, average ratio is 0.23%

Figure 4. Extension ratio and rose diagrams of the Mackenzie dyke swarm.

series of the Muskox intrusion is 1270 ± 4 Ma. Baddeleyites from four widely spaced Mackenzie dykes define a single discordia line with an upper intercept age of 1267 ± 2 Ma [*Le Cheminant and Heaman*, 1989]. The dyke age of 1267 Ma provides a time marker for much of the northwestern Canadian Shield though the geochemistry of the dykes along their trends changes because of crystal fraction [*Gibson et al.*, 1987; *Baragar et al.*, 1996].

[10] The range of Mackenzie dyke compositions match those found in the Coppermine River lava sequence. Rare earth element (REE) and other trace element abundances show a similar contraction in range, and a shift toward more evolved compositions, both upward in the lava sequence and outward along the swarm [*Baragar et al.*, 1996]. Most of the dykes that develop in different areas of the Canadian Shield do not cut each other. The Mackenzie dykes and the coeval Coppermine River lavas share similar geochemical and Nd-isotopic characteristics, and are regarded as products of the same plume [*Schwab et al.*, 2004]. This geochemical evidence suggests that the Mackenzie dyke swarm and Coppermine River lava field constitute a coeval Large Igneous Province (LIP) related to a mantle plume [*Ernst et al.*, 2005].

[11] The Mackenzie dyke swarm can be divided into two provinces based on the orientation and flow direction of the dykes. Established divisions include a radiating dyke swarm province (centered about the focal area with a radius between 400 and 600 km) and a parallel dyke swarm province (from 600 to 2100 km away from focal area). The orientation of dykes in the radiating dyke province is fan shape (rose diagrams in Figure 4), and displays a vertical flow direction [*Ernst and Baragar*, 1992], while the orientation of dykes in the parallel dyke province change from N-trending to NW-trending (normal to the Grenville Orogenic Belt) (see rose diagrams in Figure 4), and display a horizontal flow direction [*Ernst and Baragar*, 1992]. The transition from vertical to horizontal flow between 500 and 600 km from the swarm center may correspond to the outer boundary of melt generated in the mantle plume believed to be responsible for the Mackenzie igneous events. The Mackenzie dyke

swarm provides direct evidence for long-distance rapid lateral magma flow in a megaswarm, which extends hundreds of kilometers along strike [*Ernst and Baragar*, 1992].

3. Mechanics of the Mackenzie Dyke Swarm Based on Stress Field Modeling

3.1. Extension of the Canadian Shield and Emplacement of the Mafic Dyke Swarm

[12] The orientation of the stress tensor in the Earth's crust within a tectonic plate largely reflects the forces acting on that plate. Abundant information about the present-day state of intraplate stress in North America has been modeled using an elastic finite element analysis and fitted by earthquake focal mechanisms, in situ stress measurements, and borehole breakout data [*Richardson and Reding*, 1991].

[13] Mafic dyke swarms comprise quickly cooled intrusions of mafic magmas emplaced into a preexisting fracture system. The pattern of dyke swarms and the shape of individual dykes are controlled by formation mechanics of the primitive preexisting fractures. Thus, dyke swarm geometry can provide insights as to the original formation mechanics of the dyke hosting fractures [*Pollard*, 1987; *Féraud et al.*, 1987; *Ernst et al.*, 1995; *Dehls et al.*, 1998; *Acocella et al.*, 2003; *Valentine and Krogh*, 2006].

[14] The precisely dated Mackenzie dyke swarm is undeformed, unmetamorphosed, and forms a coherent pattern that can be regarded as an excellent paleostress indicator of the 1.27 Ga stress field in the Canadian Shield. The mafic dykes developed chilled margins that exhibit sharp contacts with host rocks. The Mackenzie dyke swarm is regarded as a valid marker for the 1.27 Ga crustal extension event in the Canadian Shield [*Ernst and Buchan*, 1999]. The width statistics of the Mackenzie dyke swarm on five survey lines (Figure 1) are used to estimate extension ratios of the Canadian Shield. The formula $\lambda = \Sigma d_i/(L - \Sigma d_i)$ was employed in the extension calculation, where λ is the extension ratio; Σd_i is the total width of dykes on the survey line, and L is the length of survey line across the dyke swarm. Local extension ratios were calculated and are presented in Figure 4. The extension ratio of the 1.27 Ga Canadian Shield ranges between 0.06% and 0.45% with an average extension ratio of 0.23%. The extension ratios of radiating dykes are more than those of parallel dykes in the dyke swarm. These extension ratios are much less than 1%, suggesting that the Canadian Shield experienced a brittle deformation that was recorded by the 1.27 Ga Mackenzie dyke swarm. The small magnitude of overall extension suggests that the mafic dyke swarm intruded limited elastic fractures that formed a "fracture system" in the Canadian Shield, and that the shield had become a brittle plate prior to the emplacement of the mafic dyke swarm.

3.2. Constraints on the Tectonic Model of the Mackenzie Dyke Swarm

[15] Most of the Mackenzie mafic dykes were emplaced in preexisting tensional fractures with vertical and irregular boundaries, which display stable, parallel trends not controlled by the host rock lithology [*Pollard*, 1987; *Dehls et al.*, 1998; *Acocella et al.*, 2003; *Valentine and Krogh*, 2006]. These characteristics suggest that the preexisting fracture system into which the mafic dykes intruded was formed in an extensional regional stress field or by stress concentration around a magma source. The orientations and distribution of dykes can be used to determine the nature of the paleostress field, or in defining the horizontal principal stress directions and relative magnitudes [*Price and Henry*, 1984; *Féraud et al.*, 1987; *Hoek and Seitz*, 1995; *Hou et al.*, 2006].

[16] The southern parts of the Mackenzie dyke swarm and Subdury dyke swarm terminate along the Grenville Orogen. The northern part of the Mackenzie dyke swarm terminates within the lower flows of the Coppermine River lava. The Coppermine River lava field reaches a maximum thickness of 3.5 km [*Le Cheminant and Heaman*, 1989] and extends laterally for almost 400 km and contains a volume of basaltic lava estimated at 140,000 km^3 (Figure 1). Aeromagnetic and seismic data indicate that the Coppermine River lava field underlies much of the interior platform between Great Bear Lake and the Beaufort Sea [*Le Cheminant and Heaman*, 1989].

[17] Emplacement of the Muskox intrusion was an early feature of Mackenzie magmatism. The intrusion (110 km east of Great Bear Lake on the Arctic circle) is a 125 km long, funnel-shaped body which plunges north and is therefore exposed obliquely from its southern feeder dyke to its northern roof zone [*Le Cheminant and Heaman*, 1989]. The southern edge of the preserved remnants of the Coppermine River lava field is about 400 km from the focal area for the Mackenzie dyke swarm. The Coppermine-Ekalulia basalts and Muskox intrusion were emplaced slightly prior to emplacement of the dyke swarm, with the result that subsequent mafic dyke magmas could no longer erupt through the focal area and stall at a depth of 3.5 km. Within the vertical column terminating below the focal area, the magma became feeders to volcanoes and moved through horizontally propagating dykes into preexisting fractures around the magma chamber [*Pinel and Jaupart*, 2004].

[18] The radiating dykes around the focal source were emplaced vertically, and are related to stress concentration around the magma chamber in the focal area according to the "Hole" model [*Baer and Reches*, 1991; *Pinel and Jaupart*, 2004; *Gudmundsson*, 2006] (Figure 2a). However, the model can only explain formation of small-scale radiating dyke swarms whose lengths are less than a few hundred kilometers, and cannot explain the mechanics of emplacement for the Mackenzie dyke swarm, which extends for thousands of kilometers and swings from N-S to NW-SE trending direction. The result of the "Hole" model, as calculated by *Pinel and Jaupart* [2004], is a decrease in the stress concentration magnitude with increasing radial distance from the magma chamber. At a distance equal to twice the radius of the magma chamber, the stress around the reservoir becomes negligible for the horizontal dyke propagation in the "Hole" model. The radius of the focal area of the Mackenzie dyke swarm is about 400 km, so the influence of the stress concentration around the magma chamber for the radiating dyke swarm is between 400 and 800 km, and cannot affect formation of dykes greater than 1000 km away from the magma chamber.

[19] *Rickwood* [1990] proposed a model to explain the mafic dyke swarm by lateral emplacement related to the maximum principal compressive stress orientations. In Rickwood's model, the dyke swarm has a radial distribution related to concentrated stresses around the magma chamber. With distance, dyke orientations are modified to a varying

Table 1. Mechanic Properties for Different Divisions of the Canadian Shield[a]

Division	Lithology	Young's Modulus (GPa)	Poisson's Ratio	Density (mg/cm^3)
I	2.6 Ga Archean blocks (TTG + granitoid gneiss)	80	0.25	2800
II	2.0–1.8 Ga orogen (Metavolcanics + metasemidmentary rocks, and Archean terranes)	70	0.25	2760
III	1.8–1.3 Ga subduction-related magma zone (volcanics and intrusive rocks)	40	0.23	2750

[a]*Lama and Vutukuri* [1978], *Chatterjee and Mukhopadhyay* [2002], and *Gertsch et al.* [2007].

degree by the regional stress field and the strike of the dykes bend and curve to accommodate this variation in the orientation of the net stress field [*Rickwood*, 1990; *Ernst et al.*, 1995]. In continental areas, volcanic fields exhibit long dykes in situations of horizontal emplacement [*Hildreth and Drake*, 1992; *Hildreth and Lanphere*, 1994]. *Pinel and Jaupart* [2004] studied the dynamics of horizontal dyke propagation away from the focal area of a volcanic field. They suggest that primitive magmas can no longer erupt through the focal area and stall at depth as a central cone builds up. Within a vertical column terminating below the Earth's surface, magma feeds horizontally propagating dykes. Large horizontal propagation distances can only be achieved if the volcanic stall ("Plug") prevents eruption through the focal area.

[20] After the models of *Rickwood* [1990] and *Pinel and Jaupart* [2004], we propose a "Plug" model (Figure 2b) for the Mackenzie dyke swarm. In this model, the 3.5 km thick Coppermine River lava field with 400 km radius behaves as a plug and resists the push from spreading of the Grenville Ocean along the southeast margin of the Canadian Shield (Figure 3). In the Mesoproterozoic, the southeastern margins of the Canadian Shield were active margins (Grenville Ocean), similar to the western margins of the Pacific Ocean today [*Davidson*, 1995, 1998]. Distributed ridge forces of magnitude 2.5×10^{12} N/m predict deviatoric stresses of the order of 20–40 MPa [*Richardson and Reding*, 1991; *Bott*, 1993]. Our assumption of 40 MPa deviatoric stresses acting on the southeastern margin of the Canadian Shield appears to be validated by the work of *Reynolds et al.* [2002] and *Chatterjee and Mukhopadhyay* [2002].

[21] In this "plug" model, the southern edge of the focal area (about 400 km from the focal point for magmatism) is held fixed, resisting accretionary deviatoric stresses (40 MPa) acting on the southeastern margin of the Canadian Shield during the Mesoproterozoic (Figure 3). The magnitude of overpressure in magma chambers is commonly of the order of 0.5–6 MPa [*Baer and Reches*, 1991; *Schultz*, 1995; *Gudmundsson*, 2006], much smaller than the 40 MPa and negligible in our model.

3.3. Modeling Results and Mechanics of Thin Elastic Plate

[22] The Canadian Shield was a rigid continental plate with widespread extension marked by the 1.27 Ga Mackenzie dyke swarm (Figure 1). The elastic thickness of lithosphere can be estimated by the gravity and topography data [*Bechtel et al.*, 1990; *Audet and Mareschal*, 2004; *Hoogenboom and Smrekar*, 2006], and constrained by temperature mapping [*Hyndman et al.*, 2009]. The effective elastic thickness of the Canadian Shield lithosphere is calculated to be ~100 km based on the gravity and topography of the shield, whose flexural rigidities range from about 10^{21} to 10^{25} N m^{-1} [*Bechtel et al.*, 1990; *Richardson and Reding*, 1991]. Elastic thickness of the lithosphere is able to maintain stress over long geological timescales and approximately corresponds to the depth of the 450°C isotherm. The corresponding Moho temperatures at 100 km depth are about 400°C–500°C for the Canadian Shield [*Hyndman et al.*, 2009]. These results suggest that the average elastic thickness of Canadian Shield lithosphere is about 100 km [*Audet and Mareschal*, 2004; *Hyndman et al.*, 2009]. The elastic thickness represents the part of lithosphere that behaves elastically overlying an inviscid asthenosphere. To assist detailed modeling, the Canadian Shield was subdivided into three lithologically unique provinces containing 2.6 Ga Archean blocks (I), 2.0–1.80 Ga orogenic belts (II), and 1.8–1.3 Ga subduction-related magmatic zones (III), respectively (Figure 3 and Table 1). The average mechanical properties for different units of the Canadian Shield were assumed based on these tectonic units and rocks of the Canadian Shield [*Lama and Vutukuri*, 1978; *Richardson and Reding*, 1991] (Table 1).

[23] The paleostress field can be reconstructed using linear elastic theory. A finite element model (FEM) for the shield was generated and stress trajectories were calculated by using the ANSYS 8.0 (University Version) finite element software package described by *Logan* [2007]. A more detailed description of the linear elastic finite element modeling technique can be found elsewhere [*Richardson et al.*, 1979; *Yin*, 1989, 1994; *Coblentz and Richardson*, 1995]. The 1.27 Ga stress field can be reconstructed by using a thin elastic plate finite element model based on the lithospheric characteristic of the Canadian Shield, and based on the above-outlined hypothesis for dyke orientation as an indicator of the horizontal maximum principal stress direction during dyke emplacement.

[24] The Canadian Shield was treated as a three-dimensional thin elastic plate with a thickness of about 100 km, and mechanical properties significantly different from the mantle plume and asthenosphere [*Gough et al.*, 1983; *Bechtel et al.*, 1990; *Richardson and Reding*, 1991]. The finite element grids consisted of 527 triangular elements, each defined by 6 nodes for a total of 1118 nodes. The stress trajectories of the "Plug" model for the Canadian Shield are presented in Figure 5, which is the best fit model from several tens of experiments.

[25] Best fit modeling results of paleostress fields rely on a visual fit between calculated and observed stress orientations (e.g., dyke swarm orientations) [*Yin*, 1991, 1994]. The in situ stress magnitude was not included in the calculation due to the lack of stress regime data in the observed stress indicators. The visual assessment of an FEM is to match the calculated principal stress trajectories and geological observations of dyke orientations. The errors between the dyke orientations and the maximum horizontal compressive stress orientations are less than 5° in different stress provinces of "Plug" model (Figures 1 and 5), but the errors between the orientations of dyke and stress are much greater than 30° in the margin of the

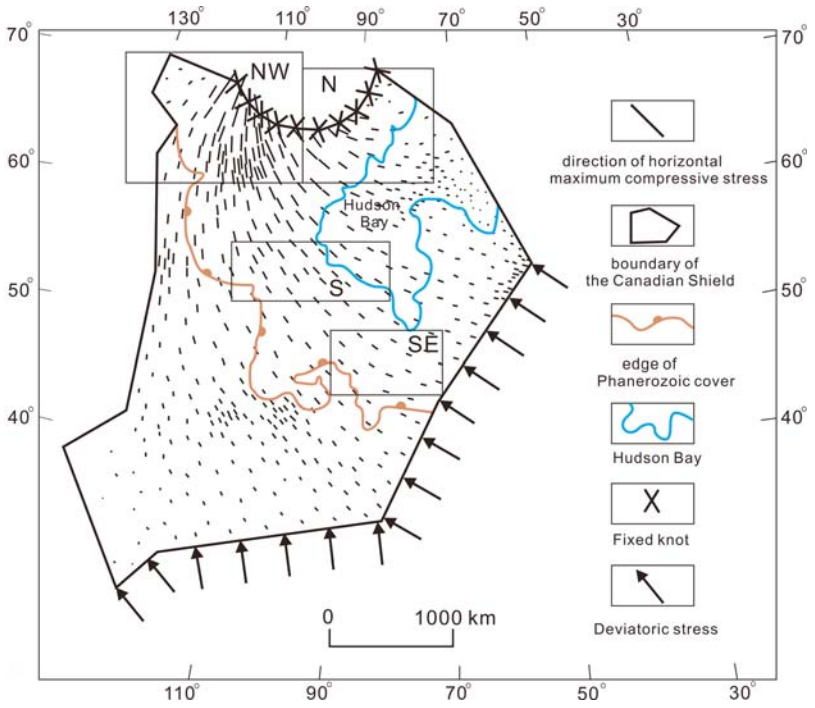

Figure 5. The horizontal maximum principal compressive stress (σ_{Hmax}) trajectory map of the Canadian Shield.

"Hole" model (Figures 1 and 2a). The modeling results of the "Plug" model are better than the "Hole" model, which yield an acceptable stress field for the 1.27 Ga Canadian Shield (Figure 5). It should be noted that, due to limitations in the resolution of gridding, the sensitivity of the modeled stresses was limited to large-scale tectonic features with wavelengths of a few tens of kilometers. Paleostress within the Canadian Shield can be divided into four stress provinces with different patterns, including: NW, N, S, and SE provinces (Figure 5). In the NW area (Slave Province), the radiating maximum horizontal compressive stresses ($\sigma_{H\mathrm{max}}$) fit well to the radiating pattern of the Mackenzie dyke swarm for which dominant orientations are N-S trending (Figures 1 and 5). In the N area, the Rae Province, the $\sigma_{H\mathrm{max}}$ orientations are NW-SE trending, and converge toward the focal area in the Coppermine River lava field (Figures 1 and 5). In the S area (the Superior Province near Hudson Bay), the $\sigma_{H\mathrm{max}}$ orientations are NW-SE trending, parallel to the orientations of the Mackenzie dyke swarm (Figures 1 and 5). In the SE area, the southern Superior Province, the $\sigma_{H\mathrm{max}}$ orientations are also NW-SE trending and parallel to the trends of the Sudbury dyke swarm [*Ernst and Buchan*, 1999] (Figures 1 and 5). Except for the southwestern Canadian Shield where the basement is covered by Phanerozoic layers, the stress trajectory map fits the orientations of dykes belonging to the Mackenzie and Sudbury dyke swarms in the different provinces (Figures 1 and 5).

[26] The modeled stress field for the 1.27 Ga Canadian Shield is shown in the horizontal maximum principal compressive stress trajectories that swing from radial (in the area surrounding the focal point) to NW-SE orientations (in the southeast), possibly due to coupling between resistance from the focal area and tectonic push acting along the southeastern margin of the Canadian Shield induced by opening of the Grenville Ocean at 1.27 Ga [*Davidson*, 1995, 1998; *Ernst and Buchan*, 1999]. The intensity of $\sigma_{H\mathrm{max}}$ orientations around the focal area (NW) is much stronger than the intensity of $\sigma_{H\mathrm{max}}$ orientations in the areas further from the focal area (to the N, S, and SE). The results also fit the developmental intensity of the Mackenzie and Sudbury dyke swarms (Figures 1 and 5). Radiating dykes correspond to the stress concentration around the magma chamber above the head of the mantle plume, but parallel dykes correspond to the regional tectonic stress field. The above-mentioned visual comparisons suggest that the "Plug" model explains the Mackenzie dyke swarm swings from radial (in the area surrounding the focal point) to NW-SE orientations (in the southeast) better than the "Hole" model that only explains the radiating pattern.

[27] Factors affecting the results of the modeling of the paleostress field include the nature of the applied tectonic forces, the shape of the Canadian Shield, the location of the magma source, and the value of the different elastic properties assigned to the Canadian Shield. The modeling results indicate that the location of the magma source and the magnitude of the deviatoric stresses applied to the southeastern margin of the shield played a dominant role in determining the paleostress field in the Canadian Shield in the Late Mesoproterozoic (Figure 5). Province boundary shapes and lithological properties also affect the stress pattern to a less degree due to the lack of significant variation in material properties across the different provinces.

[28] The distribution of stress magnitude also supports the intensity of dyke development in the Canadian Shield. The most common rocks in the shield are Precambrian granites. The Precambrian granites in the Canadian Shield are measured to have the shear stress strength of 22.8 MPa and the tensile strength of 6.78 MPa after *Gertsch et al.* [2007]. The

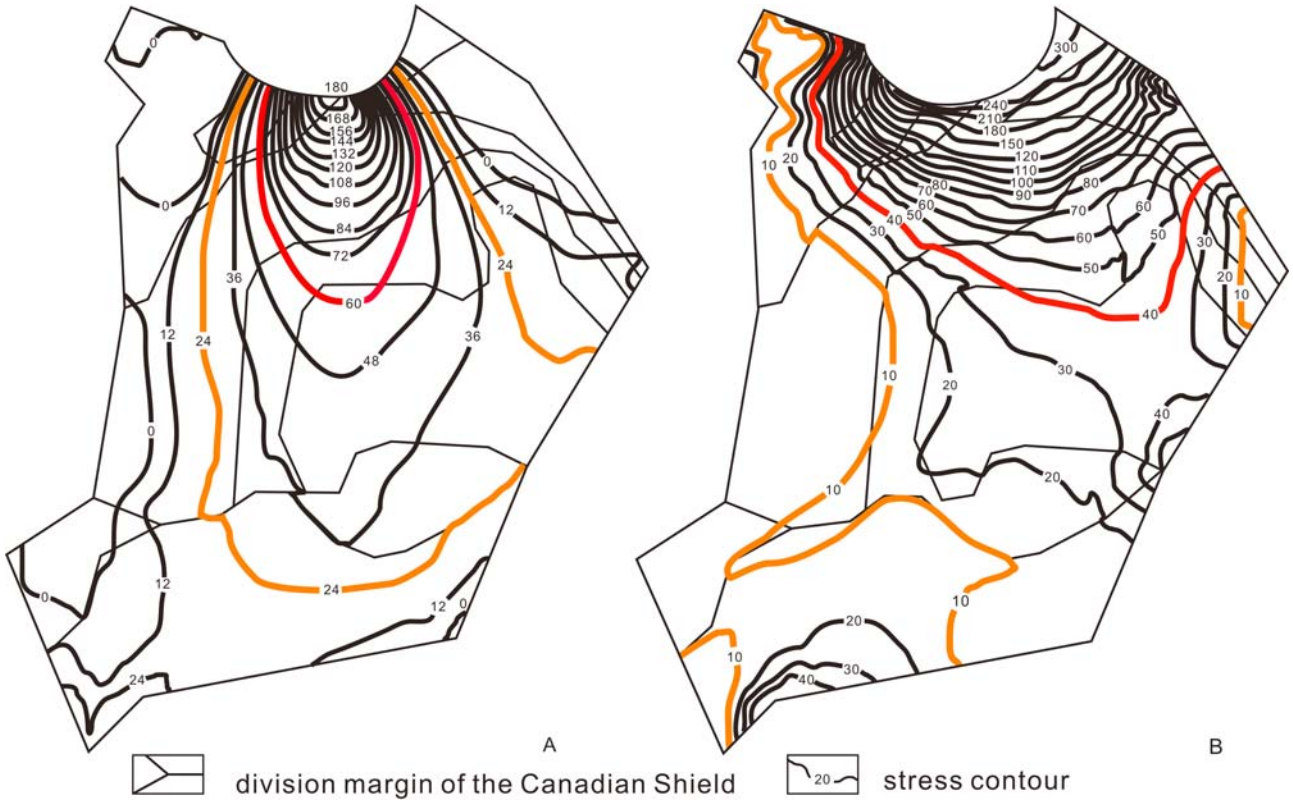

Figure 6. (a) The magnitude contours of the maximum shear stress (half deviatoric stress) in the Canadian Shield. (b) The magnitude contours of the maximum tensile stress in the Canadian Shield.

Mackenzie dyke swarm is located in the region where the magnitude of maximum shear stress (half deviatoric stress) is more than 24 MPa and the magnitude of tensile stress is more than 10 MPa (Figures 6a and 6b).

[29] Most of the dense dyke swarm is located around the focal region where the magnitude of maximum shear stress is more than 60 MPa and the magnitude of tensile stress is more than 30 MPa (Figures 6a and 6b). The predicted magnitude contour patterns of the shear and tensile stresses (higher than shear strength and tensile strength) also match the distribution of the Mackenzie dyke swarm that swings from N-S trending to NW-SE trending (from focal area to southeast margin) (Figures 6a and 6b). Few preexisting fractures of the Mackenzie dyke swarm are joint fractures, whereas most of them are tensile fractures, which typically parallel the greatest horizontal principal compressive stress [*Ernst and Baragar*, 1992; *Ernst et al.*, 1995, 2005]. The thin elastic plate at this boundary condition can generate a rather uniform distribution of tensile stress in terms of its magnitude, and produce tensile fractures that provide enough space for dyke emplacement. The contours of the stress magnitude are little affected by the rock-mechanical properties, although note that there are minor perturbations at the boundaries between regions with differing mechanical properties (Figures 6a and 6b). The modeling results based on the "Plug" model explain the observations of the radiating orientations around the magmatic focal area, and the NW-SE orientations in the southeastern Canadian Shield (Figures 1, 5, 6a, and 6b).

[30] In order to understand the properties of the thin plate model presented in this study, the effects of various models under different boundary conditions are briefly discussed to allow us to assess the uniqueness of the best fit numerical simulation discussed above. The results of the other 18 models are presented in Figure 7, including calculated horizontal maximum principal stress trajectories, contours of maximum shear and tensile stresses, and maximum error between the maximum horizontal compressive stress orientations and Mackenzie dyke swarm orientations (Figure 7). The same mechanical parameters are used for the thin plate properties of the Canadian Shield in the 14 models from Models 1–14. The different mechanical parameters of the Canadian Shield are used to discuss the influence of the mechanical properties in the other four models (Models 15–18). The calculated maximum horizontal compressive stress trajectories do not fit the orientations of the Mackenzie dyke swarm, and the maximum shear and tensile stresses are less than the shear strength (22.8 MPa) and tensile strength (6.78 MPa) in Models 1–3 (Figure 7). In Models 4 and 5, these stress trajectories also do not fit the curved pattern of the Mackenzie dyke swarm, and the regions where stress magnitudes are more than shear strength or the tensile strength do not fit the distribution of the Mackenzie dyke swarm (Figure 7). From Models 6–11, the stress trajectories of these six models do not fit the orientations of the Mackenzie dyke swarm well, though some regions where stress magnitudes are more than shear strength and tensile strength fit some portions of dyke swarm. The maximum errors between the dyke orientations and the maximum horizontal compressive stress orientations are more than 20° in these 11 models (Models 1–11 in Figure 7).

[31] The stress trajectories fit the orientations of Mackenzie dyke swarm in Models 12 and 13 quite well (maximum

Model No.	Boundary conditions	Calculated maximum horizontal compressive stress trajectories	Maximum shear stress contours	Maximum tensile stress contours	Maximal error between the dyke orientations and the maximum horizontal compressive stress orientations (±2°)
1	10 MPa magmatic overpressure is applied on the hole boundary, and four corners are fixed E=80GPa,v=0.25, ρ=2800mg/cm^3	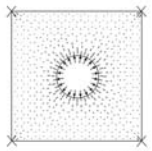	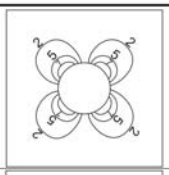	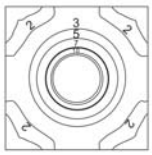	30 °
2	Hole boundary is fixed, and 40 MPa deviatoric stresses are applied on the four boundaries of square E=80GPa,v=0.25, ρ=2800mg/cm^3	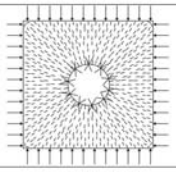	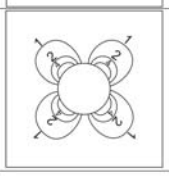	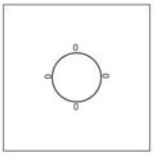	30°
3	10 MPa magmatic overpressure is applied on the upper arc boundary, and lower arc boundary is fixed E=80GPa,v=0.25, ρ=2800mg/cm^3				20°
4	Upper arc boundary is fixed, and 40 MPa deviatoric stresses are applied on the lower arc boundary E=80GPa,v=0.25, ρ=2800mg/cm^3		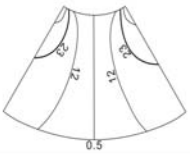	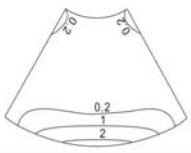	20°
5	10 MPa magmatic overpressure is applied on the north arc boundary, and the southeast boundary of the Canadian Shield is fixed E=80GPa,v=0.25, ρ=2800mg/cm^3	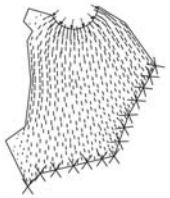			40°
6	10 MPa magmatic overpressure is applied on the north arc boundary, three nodes are fixed on the west boundary, and 40 MPa deviatoric stresses are applied on the southeast boundary of Canadian Shield E=80GPa,v=0.25, ρ=2800mg/cm^3	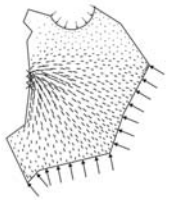	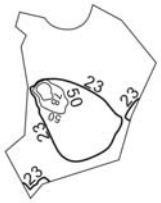	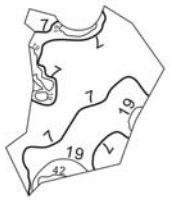	45° A

Figure 7. Comparison of model results calculating stress trajectories of the Canadian Shield.

error is less than 5° in Figure 7), but the regions where shear stress magnitudes are more than the shear strength (22.8 MPa) do not fit the curved pattern of the Mackenzie dyke swarm, though tensile stress magnitudes are more than the tensile strength (6.78 MPa) (Figure 7). In Models 14–18, the boundary of the northern arc is fixed, and 40 MPa deviatoric stresses are uniformly applied along the southeast boundary of the Canadian Shield (Figure 7). The calculated maximum horizontal compressive stress trajectories fit the orientations of Mackenzie dyke swarm well (maximum error is less than 5° in Figure 7), and the regions where stress magnitudes are more than the shear strength and tensile strength fit well to the curved pattern of the dyke swarm from north to southeast. These modeling results are very similar to the modeling result in Figure 5, but the Canadian Shield in these models is not divided into different divisions with different mechanical properties as are the models in Figure 3.

[32] The influence of rock properties in the Canadian Shield is not exactly known in searching for the best fit model. It is necessary to discuss how sensitive these models are with respect to variation of model parameters? The density ranges from 2670 kg/m^3 to 3100 kg/m^3 due to different rocks and depths in the Canadian Shield [*Audet and Mareschal*, 2004]. The Young's moduli range from 60 to 80 GPa, and the Poisson's ratios range from 0.23 to 0.25 [*Lama and Vutukuri*, 1978; *Richardson and Reding*, 1991; *Pinel and Jaupart*, 2004; *Gertsch et al.*, 2007]. In these five models (Models 14–18), different mechanical parameters are assumed within the above-mentioned value ranges. The

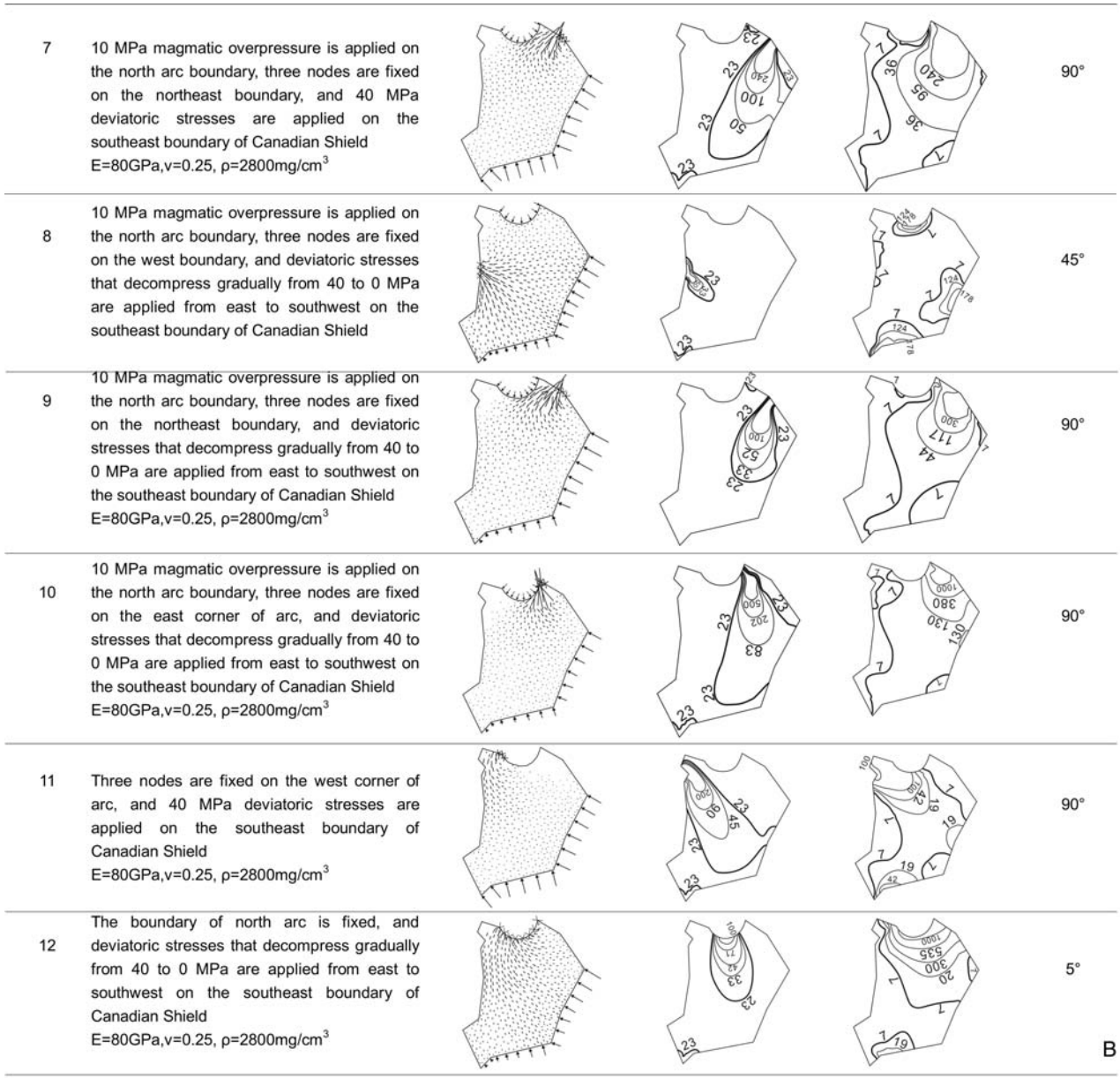

Figure 7. (continued)

calculated results suggest that the stress trajectories in these five models are much similar and fit the modeling result in Figure 5 quite well, and the regions where stress magnitudes are more than the shear strength (22.8 MPa) and tensile strength (6.78 MPa) fit the region where Mackenzie dyke swarm develops and fit the curved pattern of the dyke swarm quite well. The stress magnitude contours are much similar to each other in the five models though they have different mechanical parameters (Figure 7). It is assumed that one of the three mechanical parameters (E: Young's Modulus, ν: Poisson's ratio, ρ: Density) varies while the other two parameters remain constant during the comparison of the five models (Figure 7). These parameters little influence the stress trajectories and magnitude contour patterns. The calculated results of the five models are slightly different; for example, the region where tensile stresses are more than 30 MPa contour in Model 18 with the smallest density ($\rho = 2670$ mg/cm^3) is slightly narrower than the other models, and the region where shear stresses are more than 23 MPa contour in Model 18 is also slightly narrower than the other models. The results in these five models fit the modeling result in Figure 5 quite well though their mechanical parameters vary in the above-mentioned value ranges. It suggests that the mechanical properties are not sensitive to the in-plane traction boundary conditions in the above-mentioned value ranges (Figures 5 and 6, Models 14–18 in Figure 7).

[33] On the basis of the comparison of 18 models in Figure 7, the geometry, fixed boundary and deviatoric stresses on the boundary are sensitive to the stress trajectories. The best fit model in this study (Figure 5) suggests that interaction between the resistance of the focal area above the mantle plume and Grenville Ocean spreading played an important role in the tectonic dynamics of the Mackenzie dyke swarm.

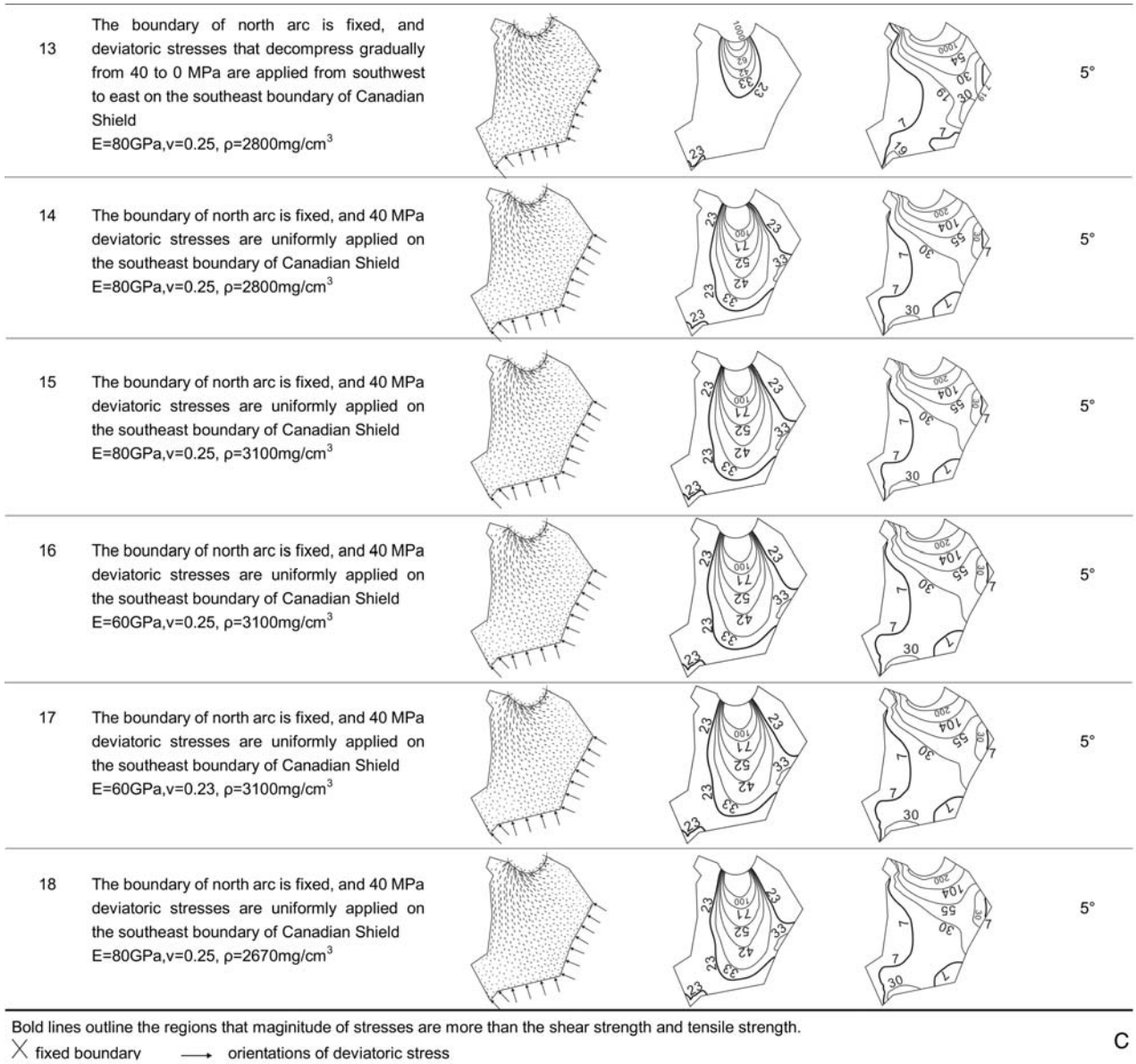

Figure 7. (continued)

3.4. Modeling Results and Mechanics of Two-Dimensional Cross Section

[34] Most large dyke swarms can be related to mantle plumes and are typically associated with divergent plate margins [*Fahrig*, 1987; *Ernst and Baragar*, 1992; *Ernst et al.*, 1995, 2005]. The focal region of the giant radiating Mackenzie dyke swarm coincides with the region of coeval volcanic and plutonic activity, and is interpreted to be located above a mantle plume [*Ernst et al.*, 1995]. The proposed tectonic model leads to questions as to what caused the emplacement of the dyke swarm. To address these questions, a two-dimensional elastic finite element model (2-D FEM) for the vertical cross-section A–J (Figures 3 and 8) across the whole Canadian Shield is also presented that examines the

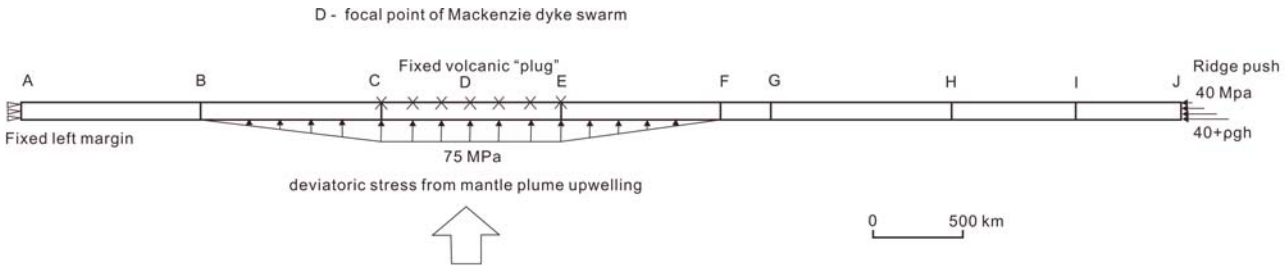

Figure 8. Two-dimensional cross-section model of the Canadian Shield.

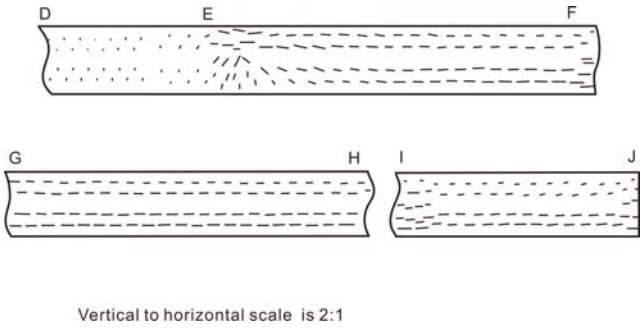

Figure 9. The maximum principal compressive stress trajectory map of the Canadian Shield cross-section vertical exaggeration × 2.

interactions among: (1) the buoyancy effect beneath the lithosphere due to the mantle plume upwelling below the focal area of the Mackenzie dyke swarm, (2) the plug effect from the volcanoes in the Coppermine River lava field, and (3) the horizontal compression from the spreading of the Grenville Ocean along the southeastern margin of the Canadian Shield, and depth-dependent stress components incorporating gravity [*Yin*, 1989, 1991, 1994].

[35] The effective elastic thickness of the Canadian Shield lithosphere is assumed to be ~100 km for the core of Precambrian continent [*Bechtel et al.*, 1990; *Richardson and Reding*, 1991]. The radius of the mantle plume below the focal region of the Mackenzie dyke swarm is assumed to be 500 km which is confirmed by the magnetic fabric data indicating that the radiating dykes were emplaced vertically in the center 500 km of the swarm, and horizontally at greater distances [*Griffiths and Campbell*, 1991; *Ernst and Baragar*, 1992]. The lithospheric stress from plume heads in the upper mantle (hot spot), from low-density asthenospheric upwelling has been modeled by finite element analysis [*Bott*, 1993]. The plume head can produce local deviatoric stresses within a plate interior region. *Bott* [1993] suggests that anomalous density between the lithosphere and the plume at the bottom of the lithosphere (about 100–400 km depths) gives rise to a deviatoric stress of 75 MPa above the buoyant load (mantle plume upwelling). In our 2-D FEM (Figure 8), a deviatoric stress of 75 MPa is assumed to act beneath the focal region with a diameter of 1000 km along the bottom of the lithosphere of the Canadian Shield. The deviatoric stress should decrease gradually from 75 to 0 MPa far away from the focal region. When magmas erupt and form lava within the focal region, primitive magmas can no longer erupt through the focal region and stall at depth (2–3 km) as a central cone builds up, and then magma has to feed horizontally propagating dykes [*Pinel and Jaupart*, 2004]. In this section model, the focal region with a diameter of 1000 km is fixed to resist the plume upwelling.

[36] In this study, it is assumed that the surface of focal area is fixed for a plug resistance to the mantle upwelling. In fact, the mantle upwelling leads to the 0.5–1 km uplift, but the uplift is usually eroded, so it is difficult to measure. The uplift is negligible relative to the thickness of lithosphere even if 1 km uplift is assumed. We suggest therefore that it is reasonable that the focal area is fixed for a plug resistance to mantle upwelling in the cross section.

[37] When a normal ocean ridge spreads, the spreading can yield a ridge push force of 2.5×10^{12} N/m referenced to old ocean floor and a deviatoric compression of about 40 MPa in old ocean floor [*Bott*, 1993]. Considering the depth-dependent stress components and incorporation of gravity, the deviatoric stresses of $40 + \rho gh$ MPa are applied to the southeastern margin of the Canadian Shield lithosphere (right margin of the section model in Figure 8). Density (ρ) is assumed to be 2750 kg/m^3, and depth (h) is assumed to be from 0 to 100 km. In the section model, the left margin is fixed at 2000 km far away from the focal region to avoid the marginal effect on the focal region (Figure 8). This is equivalent to assuming that all of the resistance to the ridge push is transmitted from the Grenville Ocean to the Canadian Shield.

[38] The mechanical properties for different units of the Canadian Shield section were assumed to be the same as the average mechanical properties of different units in the thin plate (Table 1). A finite element model (FEM) for the two-dimensional elastic section was generated and stress trajectories were calculated using the ANSYS 8.0 (University Version) finite element software package. The finite element grids consist of 668 triangular elements, each defined by three nodes for a total of 1649 nodes.

[39] The stress trajectories of the section model can be divided into three stress provinces with different patterns: vertical, horizontal, and transitional from vertical to horizontal provinces (Figure 9). The stress trajectories in the key parts of the section are presented in Figure 9. The trajectories of the maximum principal compressive stress are vertical within 500 km of the focal point of the Mackenzie dyke swarm (D and E segments of the section). The direction of the maximum principal compressive stress changes from vertical to horizontal between 500 and 600 km from the center of the swarm (outside E in Figure 9), and keeps a horhizontal direction to the south margin of Canadian Shield (from E to J, e.g., G and H and I and J segments in Figure 9). The stress trajectory patterns in different segments of the cross section are consistent with the emplacement directions of the Mackenzie dyke swarm. Magnetic fabric data indicate that magma was injected vertically within 500 km of the focal point of the dyke swarm, and then traveled horizontally at all further distances out to at least 2100 km in the Canadian Shield [*Ernst and Baragar*, 1992]. The sharp transition from vertical to horizontal flow between 500 and 600 km may correspond to the outer boundary of melt generation above the mantle plume [*Ernst and Baragar*, 1992].

[40] The magmas laterally travel large horizontal distances in preexisting fractures away from the focal area to form long dykes when a volcanic edifice prevents eruption through the focal area [*Pinel and Jaupart*, 2004; *Gudmundsson*, 2006]. Since most dykes are extensional fractures, the dykes have to horizontally propagate in a regional stress field where the maximum principal compressive stress is horizontal [*Gudmundsson*, 2006]. However, magmas rising vertically from a deep source region above a mantle plume intrude preexisting fractures to form dykes as feeders to the volcanic edifice in the focal area of radiating dyke swarm [*Ernst et al.*, 1995; *Gudmundsson*, 2006].

4. Conclusions

[41] An average extension ratio of 0.23% was calculated for the extension of the Canadian Shield based on the 1.27 Ga

Mackenzie dyke swarm. This suggests that the Canadian Shield can be assumed to have been an elastic thin plate at 1.27 Ga.

[42] Mackenzie dyke swarm is a large igneous province that intrudes the preexisting extensional fractures in a uniform stress field calculated by the "Plug" model proposed in this paper. The horizontal maximum principal compressive stress trajectories uniformly fit the orientations of the dyke swarm. Local stress concentrations around the magmatic source die out and are overwhelmed by the regional stress field with increasing distance. This causes the radial dykes to bend into parallel dykes of the swarm further from the focal source. The regional tectonic stress field is related to compressive deviarotic stresses acting on the southeast margin of Canadian Shield. The change in dyke orientation from N-S trending to NW-SE trending is caused by coupling between resistances from the focal area (Plug) and a Grenville Ocean ridge push (tectonic stress). Both orientation characteristics of the giant dyke swarm are explained by the "Plug" model, including the radiating pattern around the focal area and parallel pattern beyond the focal area.

[43] The dyke swarm is located within the magnitude contour in which the magnitude is higher than the shear strength and the tensile strength of the North American Precambrian granite. These modeling results suggest that the "Plug" model better explains the mechanics of the Mackenzie dyke swarm than the previous "Hole" model. The thin elastic plate and two-dimensional cross-section modeling suggest that the interaction between mantle plume upwelling and the Grenville Ocean spreading played an important role in the mechanics of the Mackenzie dyke swarm. Volcanoes in the focal area prevent sequential eruptions as a "Plug" above the mantle plume. The "Plug" mechanism encourages the magmas to laterally intrude the preexisting fractures beyond the focal area.

[44] The stress trajectories are continuous in the Canadian Shield due to the similar rock-mechanical properties in the different lithological provinces. This suggests that the rock-mechanical properties affect the stress trajectories less than the regional stresses. However, the contour pattern of stress magnitude is little affected by the rock-mechanical properties, although there are minor perturbations at the boundaries between regions with different mechanical properties. Magma overpressure of 0.5–6 MPa in the reservoir can be negligible, which is relative to the deviatoric stress of 75 MPa from the mantle upwelling and 40 MPa from the push of the Grenville Ocean ridge.

[45] **Acknowledgments.** We thank the five JGR reviewers including An Yin, David Giles, Taras Gerya, Trudi Hoogenboom, and an anonymous reviewer for their constructive reviews and comments that greatly improved the paper. We also thank an anonymous Associate Editor and Richard Arculus (Editor) for their helpful suggestions. We also thank Gordon S. Lister for his guidance in the Australian National University, and also offer thanks to Henry Halls for his help in the University of Toronto on this project. Xianglin Qian and Haihua Liang are also thanked for discussions relevant to this research. Thanks for Daniel Viete for going through the original manuscript word by word. Part of the work was done in the Australian National University under the ANU-PKU Exchange Project. This work was supported by funds from the National Natural Science Foundation of China Grant (40772121, 40314141, and 40172066) and China National Project 973 (2009CB219302). This paper contributes to IGCP509.

References

Acocella, V., T. Korme, F. Salvini, and R. Funiciello (2003), Elliptic calderas in the Ethiopian Rift: Control of pre-existing structures, *J. Volcanol. Geotherm. Res.*, *119*, 189–203, doi:10.1016/S0377-0273(02)00342-6.

Audet, P., and J. Mareschal (2004), Variations in elastic thickness in the Canadian Shield, *Earth Planet. Sci. Lett.*, *226*, 17–31, doi:10.1016/j.epsl.2004.07.035.

Baer, G., and M. Beyth (1990), A mechanism of dyke segmentation in fractured host rock, in *Mafic Dykes and Emplacement Mechanism*, edited by A. J. Parker, R. C. Rickwood, and D. H. Tucker, pp. 3–11, A. A. Balkema, Rotterdam, Netherlands.

Baer, G., and Z. Reches (1991), Mechanics of emplacement and tectonic implications of the Ramon Dike System, Israel, *J. Geophys. Res.*, *96*, 11,895–11,910, doi:10.1029/91JB00371.

Baragar, W. R. A., R. E. Ernst, L. Hulbert, and T. Peterson (1996), Longitudinal petrochemical variation in the Mackenzie dyke swarm, Northwestern Canadian Shield, *J. Petrol.*, *37*, 317–359, doi:10.1093/petrology/37.2.317.

Bechtel, T. D., D. W. Forsyth, V. L. Sharpton, and R. A. F. Grieve (1990), Variations in effective elastic thickness of the North American lithosphere, *Nature*, *343*, 636–638, doi:10.1038/343636a0.

Bott, M. H. P. (1993), Modelling the plate-driving mechanism, *J. Geol. Soc.*, *150*, 941–951, doi:10.1144/gsjgs.150.5.0941.

Chalmers, J. A., and K. H. Laursen (1995), Labrador Sea: The extent of continental and oceanic crust and the timing of the onset of seafloor spreading, *Mar. Pet. Geol.*, *12*(2), 205–206, doi:10.1016/0264-8172(95)92840-S.

Chatterjee, R., and M. Mukhopadhyay (2002), Effects of rock mechanical properties on local stress field of the Mahanadi basin, India—Results from finite element modelling, *Geophys. Res. Lett.*, *29*(11), 1533, doi:10.1029/2001GL013447.

Coblentz, D. D., and R. M. Richardson (1995), Statistical trends in the intraplate stress field, *J. Geophys. Res.*, *100*(B10), 20,245–20,255.

Davidson, A. (1995), A review of the Grenville orogen in its North American type area, *AGSO J. Aust. Geol. Geophys.*, *16*, 3–24.

Davidson, A. (1998), An overview of Grenville Province geology, Canadian Shield, in *Geology of the Precambrian Superior and Grenville Provinces and Precambrian Fossils in North America*, *Geol. Can.*, vol. 7, edited by S. B. Lucas and M. St-Onge, chap. 3, pp. 205–270, Geol. Surv. of Canada, Ottawa, Ontario, Canada.

Dehls, J. F., A. R. Cruden, and J. L. Vigneresse (1998), Fracture control of late Archean pluton emplacement in the northern Slave Province, Canada, *J. Struct. Geol.*, *20*, 1145–1154, doi:10.1016/S0191-8141(98)00055-8.

Ernst, R. E., and W. R. A. Baragar (1992), Evidence from magnetic fabric for the flow pattern of magma in the Mackenzie giant radiating dyke swarm, *Nature*, *356*, 511–513, doi:10.1038/356511a0.

Ernst, R. E., and K. L. Buchan (1999), Paleo-stress pattern from giant dyke swarms, *Lunar Planet. Sci.*, *30*, 1737–1738.

Ernst, R. E., J. W. Head, E. Parfitt, E. Grosfils, and L. Wilson (1995), Giant radiating dyke swarms on Earth and Venus, *Earth Sci. Rev.*, *39*, 1–58, doi:10.1016/0012-8252(95)00017-5.

Ernst, R. E., K. L. Buchan, and I. H. Compbell (2005), Frontiers in Large Igneous Province research, *Lithos*, *79*, 271–297, doi:10.1016/j.lithos.2004.09.004.

Fahrig, W. F. (1987), The tectonic settings of continental mafic dyke swarms: Failed arm and early passive margin, in *Mafic Dyke Swarms*, edited by H. C. Halls and W. F. Fahrig, *Geol. Assoc. Can. Spec. Pap., 34*, 331–348.

Féraud, G., G. Giannérini, and R. Campredon (1987), Dyke swarms as paleostress indicators in areas adjacent to continental collision zones: Examples from the European and northwest Arabian Plates, in *Mafic Dyke Swarms*, edited by H. C. Halls and W. F. Fahrig, *Geol. Assoc. Can. Spec. Pap., 34*, 273–278.

Gertsch, R., L. Gertsch, and J. Rostami (2007), Disc cutting tests in Colorado Red Granite: Implications for TBM performance prediction, *Int. J. Rock Mech. Min. Sci.*, *44*, 238–246, doi:10.1016/j.ijrmms.2006.07.007.

Gibson, I. L., N. S. Madhurendra, and W. F. Fahrig (1987), The geochemistry of the Mackenzie dyke swarm, Canada, in *Mafic Dyke Swarms*, edited by H. C. Halls and W. F. Fahrig, *Geol. Assoc. Can. Spec. Pap., 34*, 457–465.

Gough, D. I., C. K. Fordjor, and J. S. Bell (1983), A stress province boundary and tractions on the North American plate, *Nature*, *305*, 619–621, doi:10.1038/305619a0.

Gower, C. F., A. B. Ryan, and T. Rivers (1990), Mid-Proterozoic Laurentia-Baltic: An overview of its geological evolution and summary of the contributions by this volume, in *Mid-Proterozoic Laurentia-Baltica*, edited by C. F. Gower, T. Rivers, and B. Ryan, *Geol. Assoc. Can. Spec. Pap., 38*, 1–20.

Griffiths, R. W., and I. H. Campbell (1991), Interaction of mantle plume heads with the Earth's surface and onset of small-scale convection, *J. Geophys. Res.*, *96*, 18,295–18,310, doi:10.1029/91JB01897.

Grover, T. W., D. R. M. Pattison, M. R. McDonough, and V. J. McNicoll (1997), Tectonometamorphic evolution of the southern Talson magmatic

zone and associated zones, Northeastern Alberta, *Can. Mineral.*, *35*, 1051–1067.

Gudmundsson, A. (1995), The geometry and growth of dykes, in *Physics and Chemistry of Dykes*, edited by G. Baer and A. Heimann, pp. 23–34, A. A. Balkema, Rotterdam, Netherlands.

Gudmundsson, A. (2002), Emplacement and arrest of sheets and dykes in central volcanoes, *J. Volcanol. Geotherm. Res.*, *116*, 279–298, doi:10.1016/S0377-0273(02)00226-3.

Gudmundsson, A. (2006), How local stresses control magma-chamber ruptures, dyke injections, and eruptions in composite volcanoes, *Earth Sci. Rev.*, *79*, 1–31, doi:10.1016/j.earscirev.2006.06.006.

Heeremans, M., B. Larsen, and H. Stel (1996), Paleostress reconstruction from kinematic indicators in the Oslo Graben, southern Norway: New constraints on the mode of rifting, *Tectonophysics*, *266*, 55–79, doi:10.1016/S0040-1951(96)00183-7.

Hildreth, W., and R. E. Drake (1992), Volcan Quizapu, Chilean Andes, *Bull. Volcanol.*, *54*, 93–125, doi:10.1007/BF00278002.

Hildreth, W., and M. A. Lanphere (1994), Potassium-argon geochronology of a basalt-andesite-dacite arc system: The Mount Adams volcanic field, Cascade Range of southern Washington, *Geol. Soc. Am. Bull.*, *106*, 1413–1429, doi:10.1130/0016-7606(1994)106<1413:PAGOAB>2.3.CO;2.

Hoek, J. D., and H. M. Seitz (1995), Continental mafic dyke swarms as tectonic indicators: An example from the Vestfold Hills, East Antarctica, *Precambrian Res.*, *75*, 121–139, doi:10.1016/0301-9268(95)00033-X.

Hoffman, P. F. (1989), Precambrian geology and tectonic history of North America, in *The Geology of North America: An Overview*, edited by A. W. Bally and A. R. Palmer, pp. 447–512, Am. Geol. Soc., Boulder, Colo.

Hoffman, P. F. (1991), Did the breakout of Laurentia turn Gondwana inside out?, *Science*, *252*, 1409–1412, doi:10.1126/science.252.5011.1409.

Hoogenboom, T., and S. E. Smrekar (2006), Elastic thickness estimates for the northern lowlands of Mars, *Earth Planet. Sci. Lett.*, *248*, 830–839, doi:10.1016/j.epsl.2006.06.035.

Hou, G.-T., C.-C. Wang, J.-H. Li, and X.-L. Qian (2006), Late paleoproterozoic extension and a paleostress field reconstruction of the North China craton, *Tectonophysics*, *422*, 89–98, doi:10.1016/j.tecto.2006.05.008.

Hyndman, R. D., C. A. Currie, S. Mazzotti, and A. Frederiksen (2009), Temperature control of continental lithosphere elastic thickness, *Te* vs *Vs*, *Earth Planet. Sci. Lett.*, *277*, 539–548, doi:10.1016/j.epsl.2008.11.023.

Karlstrom, K. E., S. S. Harlan, K. I. Åhäll, M. L. Williams, J. McLelland, and J. W. Geissman (2001), Long-lived (1.8–1.0 Ga) convergent orogen in southern Laurentia, its extensions to Australia and Baltica, and implications for refining Rodinia, *Precambrian Res.*, *111*, 5–30, doi:10.1016/S0301-9268(01)00154-1.

Kusky, T. M., and D. P. Loring (2001), Structural and U/Pb chronology of superimposed folds, Adirondack Mountains: Implications for the tectonic evolution of the Grenville province, *J. Geodyn.*, *32*, 395–418, doi:10.1016/S0264-3707(01)00038-2.

Kusky, T. M., and A. Polat (1999), Growth of granite-greenstone terranes at convergent margins, and stabilization of Archean cratons, *Tectonophysics*, *305*, 43–73, doi:10.1016/S0040-1951(99)00014-1.

Kusky, T. M., and J. Vearncombe (1997), Structure of Archean Greenstone Belts, in *Tectonic Evolution of Greenstone Belts*, edited by M. J. De Wit and L. D. Ashwal, chap. 3, pp. 95–128, Oxford Univ. Press, Oxford, U. K.

Lama, R. D., and V. S. Vutukuri (Eds.) (1978), Testing techniques and result, in *Handbook on Mechanical Properties of Rocks*, vol. 2, pp. 315–453, Trans Tech., Zurich, Switzerland.

Le Cheminant, A. N., and L. M. Heaman (1989), Mackenzie igneous events, Canada: Middle Proterozoic hotspot magmatism associated with ocean opening, *Earth Planet. Sci. Lett.*, *96*, 38–48, doi:10.1016/0012-821X(89)90122-2.

Logan, D. L. (Ed.) (2007), *A First Course in the Finite Element Method*, 4th ed., 752 pp., Brooks/Cole, Pacific Grove, Calif.

Park, R. G. (1992), Plate kinematic history of Baltica during the middle to late Proterozoic: A model, *Geology*, *20*, 725–728, doi:10.1130/0091-7613(1992)020<0725:PKHOBD>2.3.CO;2.

Pinel, V., and C. Jaupart (2004), Magma strorage and horizontal dyke injection beneath a volcanic edifice, *Earth Planet. Sci. Lett.*, *221*, 245–262, doi:10.1016/S0012-821X(04)00076-7.

Pollard, D. D. (1987), Elementary fractures mechanics applied to the structural interpretation of dykes, in *Mafic Dyke Swarms*, edited by H. C. Halls and W. H. Fahrig, *Geol. Assoc. Can. Spec. Pap., 34*, 5–24.

Price, J. G., and C. D. Henry (1984), Stress orientations during Oligocene volcanism in Trans-Pecos Texas: Timing the transition from Laramide compression to basin and range tension, *Geology*, *12*, 238–241, doi:10.1130/0091-7613(1984)12<238:SODOVI>2.0.CO;2.

Reynolds, S. D., D. D. Coblentz, and R. R. Hillis (2002), Tectonic forces controlling the regional intraplate stress field in continental Australia: Results from new finite element modeling, *J. Geophys. Res.*, *107*(B7), 2131, doi:10.1029/2001JB000408.

Richardson, R. M., and L. M. Reding (1991), North American plate dynamics, *J. Geophys. Res.*, *96*(12), 201–212, 223.

Richardson, R. M., S. C. Solomon, and N. H. Sleep (1979), Tectonic stress in the plates, *Rev. Geophys.*, *17*(5), 981–1019, doi:10.1029/RG017i005p00981.

Rickwood, P. C. (1990), The anatomy of a dyke and the determination of propagation and magma flow directions, in *Mafic Dykes and Emplacement Mechanisms*, edited by A. J. Parker, P. C. Rickwood, and D. H. Tucker, pp. 81–100, A. A. Balkema, Rotterdam.

Roest, W. R., and S. P. Srivistava (1989), Sea-floor spreading in the Labrador Sea: A new reconstruction, *Geology*, *17*, 1000–1003, doi:10.1130/0091-7613(1989)017<1000:SFSITL>2.3.CO;2.

Schultz, R. A. (1995), Limits on strength and deformation properties of jointed basaltic rock masses, *Rock Mech. Eng.*, *28*, 1–15, doi:10.1007/BF01024770.

Schwab, D. L., D. J. Thorkelson, J. K. Mortensen, R. A. Creaser, and J. G. Abbott (2004), The Bear River dykes (1265–1269 Ma): Westward continuation of the Mackenzie dyke swarm into Yukon, Canada, *Precambrian Res.*, *133*(3–4), 175–186, doi:10.1016/j.precamres.2004.04.004.

Smith, R. P. (1987), Dyke emplacement at Spanish Peaks, Colorado, in *Mafic Dyke Swarms*, edited by H. C. Halls and W. F. Fahrig, *Geol. Assoc. Can. Spec. Pap., 34*, 47–54.

Valentine, G. A., and K. E. C. Krogh (2006), Emplacement of shallow dikes and sills beneath a small basaltic volcanic center: The role of pre-existing structure (Paiute Ridge, southern Nevada, USA), *Earth Planet. Sci. Lett.*, *246*, 217–230, doi:10.1016/j.epsl.2006.04.031.

Van Kranendonk, M. J., M. R. St-Onge, and J. R. Henderson (1993), Paleoproterozoic tectonic assembly of North Laurentia through multiple indentations, *Precambrian Res.*, *63*, 325–347, doi:10.1016/0301-9268(93)90039-5.

Windley, B. (1992), Proterozoic collisional and accretional orogens, in *Proterozoic Crustal Evolution*, edited by K. C. Condie, pp. 419–446, Elsevier, Amsterdam.

Yin, A. (1989), Origin of regional, rooted low-angle normal faults: A mechanical model and its tectonic implications, *Tectonics*, *8*, 469–482, doi:10.1029/TC008i003p00469.

Yin, A. (1991), Mechanisms for the formation of domal and basinal detachment faults: A three-dimensional analysis, *J. Geophys. Res.*, *96*, 14,577–14,594.

Yin, A. (1994), Mechanics of monoclinal systems in the Colorado Plateau during the Laramide Orogeny, *J. Geophys. Res.*, *99*, 22,043–22,058.

G. Hou, C. Wang, and Y. Wang, Key Laboratory of Orogenic Belts and Crustal Evolution, School of Earth and Space Sciences, Peking University, Beijing 100871, China.

T. M. Kusky, Three Gorges Geohazards Research Center, China University of Geosciences, Wuhan 430074, China. (gthou@pku.edu.cn)